Nuclear Instruments and Methods in Physics Research A 1068 (2024) 169757

Contents lists available at ScienceDirect

Nuclear Inst. and Methods in Physics Research, A

journal homepage: www.elsevier.com/locate/nima

Experimental qualification and modelling of the non-linear response of the DEPFET active pixel sensor for the DSSC camera

Andrea Castoldi [a,b,*], Maurizio Ghisetti [a,b], Chiara Guazzoni [a,b], Stefan Aschauer [c], Lothar Strüder [c], Karsten Hansen [d], Stefano Maffessanti [d], Matteo Porro [e,f]

[a] Politecnico di Milano, DEIB, Piazza Leonardo da Vinci 32, 20133, Milano, Italy
[b] INFN, Sezione di Milano, Via Celoria 16, 20133, Milano, Italy
[c] PNSensor GmbH, Otto-Hahn-Ring 6, 81739, Munich, Germany
[d] Deutsches Elektronen-Synchrotron DESY, Notkestraße 85, 22607, Hamburg, Germany
[e] European XFEL, Holzkoppel 4, 22869, Schenefeld, Germany
[f] Universita' Ca' Foscari Venezia, Dipartimento di Scienze Molecolari e Nanosistemi, Via Torino 155, 30170, Venezia, Italy

ARTICLE INFO

Keywords:
Ultra-fast X-ray imaging
DEPFET
Non-linear response
XFEL

ABSTRACT

A modified Depleted P-Channel Field Effect Transistor (DEPFET) is the key feature of the DEPFET Sensor with Signal Compression (DSSC), a 1 Mpixel X-ray camera aiming at ultra-fast imaging of soft X-rays at the European XFEL. Operation of large-area devices with a large number of DSSC-type DEPFET pixels requires the accurate knowledge of the sensitivity of the response to the relevant DEPFET parameters. The paper presents the experimental qualification of the response of DSSC-type DEPFET pixels in the space of 4 relevant parameters: drain current, source voltage, drain voltage and back side voltage. The obtained results allow estimation of the impact of the inevitable parameter fluctuations in large monolithic sensors and of the actual trimming range of the shape of signal compression in view of the pixelwise calibration of the 1 Mpixel DSSC camera.

1. Introduction

Active pixel sensors based on the Depleted P-Channel Field Effect Transistor (DEPFET) feature excellent spectroscopic performance thanks to the small capacitance of the sense node and are unique devices that can achieve high-speed X-ray imaging down to few hundreds of eV photon energy when combined with a suitable technology of the entrance window [1]. The DEPFET active pixel consists in integrating a MOSFET on a high resistivity n-doped silicon bulk with a deep n-implant below the channel (internal gate). Signal electrons collected in the internal gate cause an increase of channel conductivity and of the DEPFET current, with amplification defined as $g_q = \Delta I_{drain}/Q_{signal}$. A modified design of the DEPFET with non-linear (NL) response has been proposed [2] to cope with the demanding dynamic range requirements of photon detectors at the novel Free Electron Laser sources and is the key feature of the 1 Mpixel DEPFET Sensor with Signal Compression (DSSC) [3], aiming at ultra-fast imaging of soft X-rays at the European XFEL [4]. The compression mechanism of the DEPFET response is obtained by extending the internal gate underneath the source contact, where the electrostatic coupling to the DEPFET channel is weaker. As a consequence, at increasing signal levels the signal charge progressively spreads towards the source, giving rise to the desired compression shape. The DEPFET pixels with NL response have been already demonstrated [5] and large-area monolithic active pixel sensors (128 x 256 pixels) with DSSC-style DEPFETs have been produced with a custom 0.35 μm CMOS process.

Operation of large-area devices with a large number of DSSC-type DEPFETs requires, however, to study in detail the sensitivity of the NL response to all relevant parameters. The main open issues to be investigated are the following: (i) the impact of voltage drops of the drain and source supply voltages of the DEPFET, (ii) the possibility to adjust the shape of the NL response, (iii) the impact of a change of the back voltage, influenced by bulk doping and by the level of leakage current. To this purpose we conducted an experimental qualification of DSSC-type DEPFET pixels to investigate the sensitivity of the NL response in the space of 4 relevant parameters: drain current, source voltage, drain voltage and back side voltage.

2. Experimental setup and method

The tested DEPFET pixels are arranged in a 7-cell cluster fabricated on a 725 μm thick high-resistivity silicon wafer processed in a custom

* Corresponding author at: Politecnico di Milano, DEIB, Piazza Leonardo da Vinci 32, 20133, Milano, Italy.
E-mail address: andrea.castoldi@polimi.it (A. Castoldi).

https://doi.org/10.1016/j.nima.2024.169757
Received 27 June 2024; Received in revised form 25 July 2024; Accepted 18 August 2024
Available online 19 August 2024

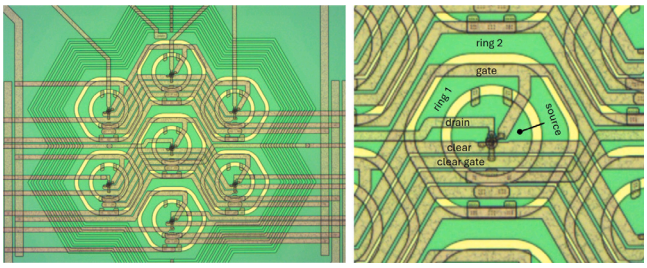

Fig. 1. Layout of the tested DEPFET pixels. (left) 7-cell structure. (right) Detail of the central pixel. The side of the hexagonal pixel is 136 μm. The gate length of the DEPFET is 2 μm and the gate width is about 16 μm.

double-sided 0.35 μm CMOS-DEPFET technology. The technology and geometrical size of the DEPFET pixels are the same as the ones of the DSSC detector. The layout of the tested structure is shown in Fig. 1. The 7-cell structure is bonded to a ceramic board connected via a ZIF socket to the mainboard which distributes the required static and dynamic supply voltages. The DEPFET current is readout (drain readout configuration) by a transimpedance amplifier (TIA) followed by an external 14-bit ADC providing a resolution of the DEPFET current of the order of 1 nA.

Qualification of the NL response curve of the DEPFET requires injection of an increasing amount of calibrated charge into the internal gate. However, the DSSC-type pixels feature a thin Al layer on the back side as a light-blocking filter requested by European XFEL instruments which generally prevents injection of the signal charge with a standard pulsed optical laser (tests with a dedicated setup for laser injection are reported in [6]). As an alternative method, we used the thermally-generated leakage current in the pixel to scan the NL DEPFET response. The leakage current in the DEPFET pixel is independent of the fill level of the internal gate, therefore the accumulated charge ΔQ_{int} is solely proportional to the integration time. Fig. 2 shows the measurement sequence. After the removal of the signal charge stored in the internal gate (reset), the integration of the leakage current in the internal gate starts and the baseline is sampled. Samples of the signal are acquired at equal time intervals, t_{int}, to scan the DEPFET response. To avoid drifts in the operating conditions we conducted all measurements at controlled temperature ($-20\ ^{\circ}C$). The granularity of the scan is related to the integration time and to the level of leakage current in the pixel (typically $<10\,fA$). A complete measurement scan of the response up to about 1.5 MeV deposited energy takes several seconds (≈1000 points). The back side was biased at −200 V and the drift rings 1 and 2 were biased at −10 V and −20 V, respectively. Absolute calibration of the DEPFET current is done by injection of a known current via a resistor and thus calibrating the TIA gain. The acquisition of ^{55}Fe spectra – per pixel and for every tested condition – allowed calibration of the injected charge per integration time exploiting the linear portion of the DEPFET response. Calibration errors are related to spectra peak fitting (pedestal, injected charge peak and Mn Kα line) and are typically of ≈1%.

3. Fitting model

An example of the measured signal current as a function of the deposited energy is shown in Fig. 3(a). The slope of the signal current represents the gain (i.e. charge-to-current amplification of the DEPFET) that is shown in Fig. 3(b). The DSSC-type DEPFET response features three compression "kinks", corresponding to three overflow regions under the source. The plot of the gain better reveals the details of the corresponding gain "steps". We modelled a single gain step with the function:

$$H(E, E_a, E_b, n) = \left[\frac{1+\left(\frac{E^2}{E_b^2}\right)^n}{1+\left(\frac{E^2}{E_a^2}\right)^n}\right]^{\frac{1}{2}}$$

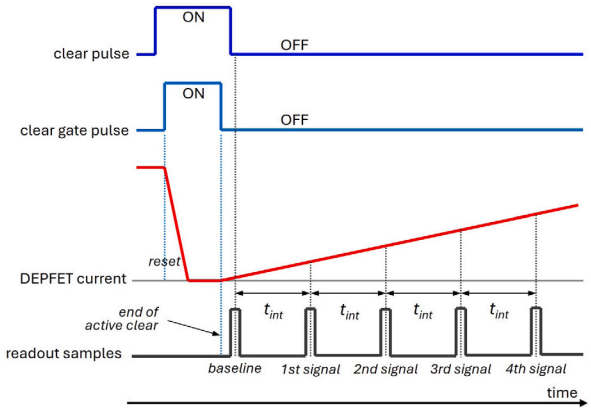

Fig. 2. Measurement sequence to scan the DEPFET NL response using the pixel leakage current.

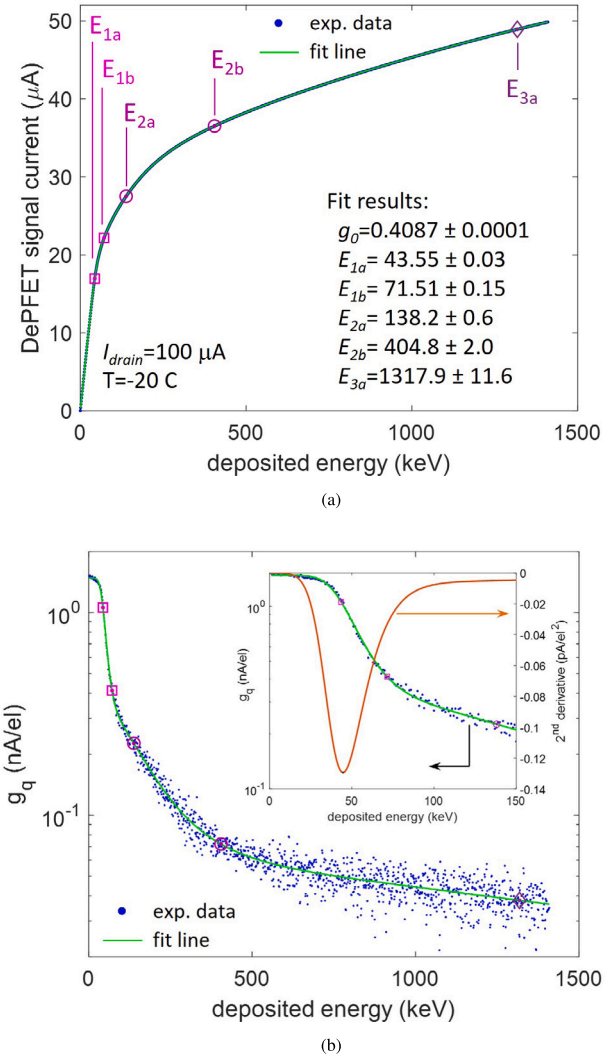

Fig. 3. Measured DEPFET response vs. the deposited energy (V_{source} = 0 V, V_{drain} = −4 V, I_{drain} = 100 μA). (a) Signal current. The estimated values of relevant fit variables are shown (E_{ia}, E_{ib} refer to the ith gain step). (b) DEPFET gain. The inset shows a zoomed view. The 2nd derivative of the signal current, whose minimum defines the onset of the kink transition, is also shown.

where E_a, E_b define the kink transition region and n is correlated to the gain ratio (or compression factor). The gain function can be

extended to any number of gain steps and the final custom fit function for the DEPFET signal current is obtained by numerical integration of the gain model. An example of the obtained fit results is given in Fig. 3. As the 3rd kink is always outside the tested range ($E \ll E_{3b}$), the function of the 3rd gain step is simplified by retaining only the E_{3a} term. The fitting model nicely catches all the features of the DEPFET response with excellent Goodness-of-fit indicators (RMSE≈0.02 ADU, adjusted R-squared = 1.0000) and with standard errors of the estimated fit parameters below 1%. The inset of Fig. 3(b) shows the detail of the first gain step and the 2nd derivative of the signal current that identifies the onset energy of the kink transition. Another parameter of interest is the compression factor, i.e. the ratio between the gain in the linear region and at high energies, that tends asymptotically to an energy-independent value.

4. Results and discussion

Three measurement sweeps of the DEPFET parameters (I_{drain}, V_{source}, V_{drain}) were carried out. Starting from the reference bias condition $V_{source} = 0$ V, $V_{gate} = -2.58$ V, $V_{drain} = -4$ V and $I_{drain} = 150$ μA, one variable is swept while the independent variables are kept at the reference value. The DEPFET bias conditions of the 3 sweeps are summarized below.

- Drain current sweep: I_{drain} from 50 μA to 150 μA, steps of 10 μA (V_{gate} changes from −1.51 V to −2.58 V). $V_{source} = 0$ V, $V_{drain} = -4$ V.
- Source voltage sweep: V_{source} from 0 V to −0.5 V, steps of 0.1 V (I_{drain} changes from 147 μA to 78 μA). $V_{gate} = -2.58$ V, $V_{drain} = -4$ V.
- Drain voltage sweep: V_{drain} from −4.5 V to −3 V, steps of 0.5 V (V_{gate} changes from −2.46 V to −2.87 V). $I_{drain} = 147$ μA, $V_{source} = 0$ V.

Fig. 4(a) shows DEPFET signal current curves versus the deposited energy when I_{drain} is swept from 50 μA to 150 μA. At the reference bias condition ($I_{drain} = 150$ μA), the DEPFET gain g_q changes with deposited energy from 1.57 nA/el (linear region) to 45.6 pA/el (at 1 MeV), corresponding to a compression factor of 34.4. The signal current grows with I_{drain} as a result of the change of the DEPFET gain and of the kink transition regions. The gain g_q in the linear region, plotted in Fig. 4(b), grows with I_{drain} which explains the increase of the signal current as well as the increase of the global compression factor (Fig. 5, bottom).

The impact of the DEPFET voltages on the 1st kink transition region, defining the extension of the region of linear amplification, is analysed in Fig. 5 (top). Here the fit variables E_{1a}, E_{1b} are plotted together with the onset energy of signal compression. V_{source} and V_{drain} have significant impact on the 1st kink energy due to the stronger electrostatic coupling between the internal gate and the DEPFET channel. In particular, V_{drain} can trim the 1st kink energy from about 34 keV to 63 keV. Fig. 5 (bottom) shows the compression factor, which varies between 32 and 36 in the explored variable range.

The impact of the back side voltage (V_{back}) on the DEPFET signal current has also been tested on different DEPFET structures (gate length ≈3.5 μm and gate width ≈40 μm) fabricated on a thinner substrate (450 μm). Changing V_{back} in the range [−80 V, −150 V] has no impact on the linear region of the response, while at higher energy the signal current increases with the reverse voltage. This trend is explained by the increase of the potential barrier between the internal gate and the overflow region, connected to the increase of the 1st kink energy, resulting from the different capacitive partition of the change of the reverse voltage. As a reference, at 230 keV the sensitivity of the signal current to the back voltage was found 32.4 nA/V. Although tested on a different substrate thickness, the measured sensitivity to the back side voltage confirms the impact on the extension of the linear region and on the shape of the response.

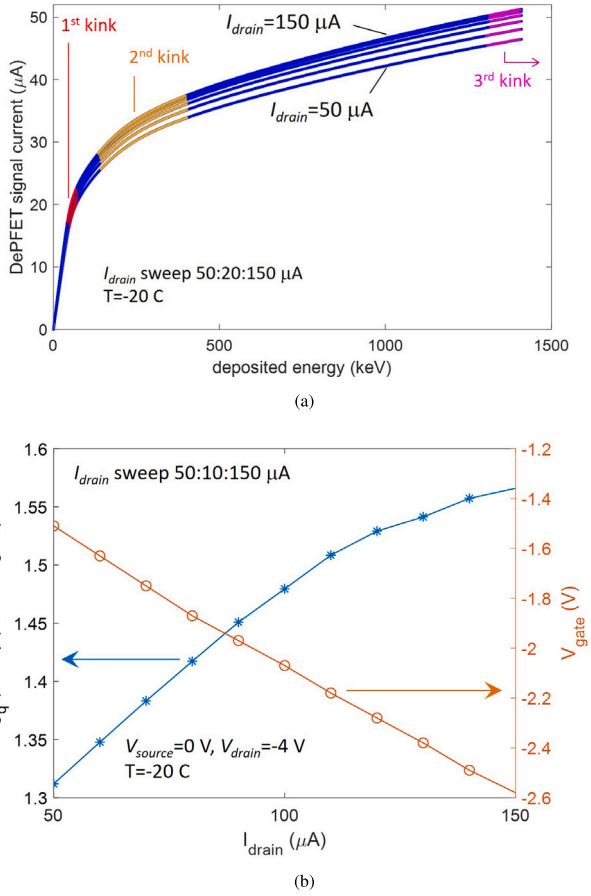

Fig. 4. Impact of I_{drain} on the DEPFET response. (a) DEPFET signal current vs deposited energy. Kink transition regions are indicated. (b) DEPFET gain (linear region) and gate voltage as a function of the drain current.

5. Conclusions and outlook

Measurement sweeps of the main relevant DEPFET parameters (I_{drain}, V_{source}, V_{drain}, V_{back}) were carried out to assess the sensitivity of the DEPFET response to the inevitable parameter fluctuation expected in large monolithic sensors and to investigate the trimming range. The fit function proved to accurately model the DEPFET response and it will be a precious tool for calibration as it allows reduction of the number of experimental points, resampling and efficient parametrization of the NL pixel response (e.g. 9 parameters/pixel in the studied case) [7]. The measurement technique, based on the integration of the leakage current, allowed to nicely scan the DSSC response up to about 1.5 MeV and is potentially applicable to the 1 Mpixel DSSC camera. Further investigation on the dispersion of leakage current in large arrays and on the maximum useable measurement time must be carried out. The results show that the DEPFET pixel was always functional within the range of the tested variables and confirmed the possibility to adjust the shape of the response before the final pixelwise calibration of the 1 Mpixel DSSC camera.

Declaration of competing interest

The authors declare that they have no known competing financial interests or personal relationships that could have appeared to influence the work reported in this paper.

Acknowledgment

This work has been carried out in the framework of the DSSC project funded by the European XFEL.

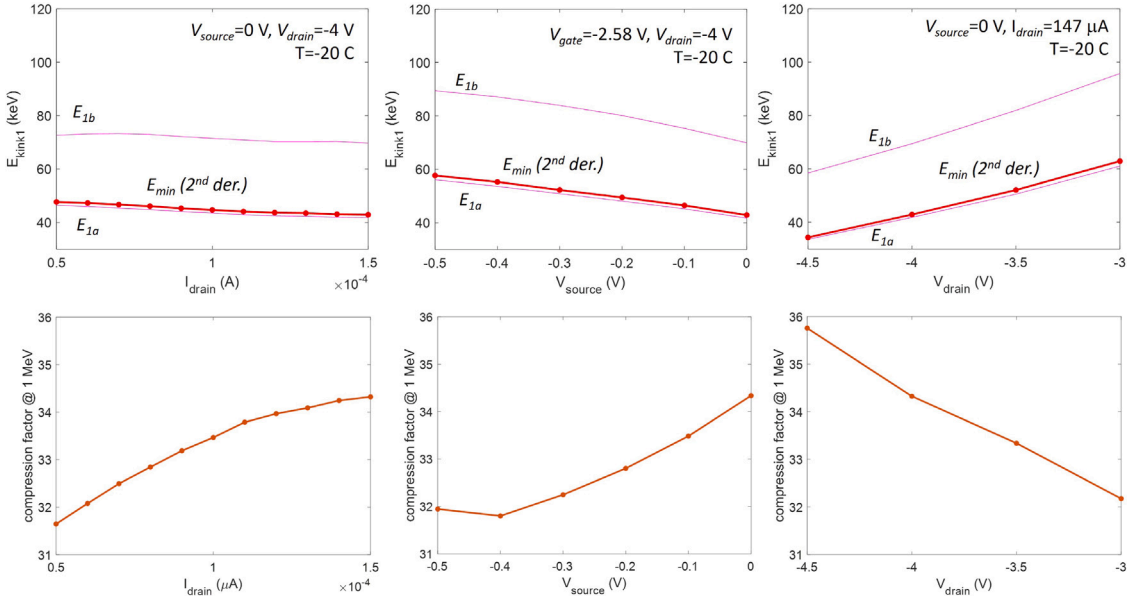

Fig. 5. Summary results of the 3 measurement sweeps (I_{drain}, V_{source}, V_{drain}). The top figures show the sensitivity of the 1st kink region (fit variables E_{1a}, E_{1b} and onset energy of the 1st kink, E_{min}) to the sweep variable. The bottom figures show the corresponding compression factors at 1 MeV.

References

[1] L. Andricek, A. Bähr, P. Lechner, J. Ninkovic, R. Richter, F. Schopper, J. Treis, DePFET—Recent developments and future prospects, Front. Phys. 10 (2022) 1–10, http://dx.doi.org/10.3389/fphy.2022.896212.

[2] G. Lutz, P. Lechner, M. Porro, L. Strüder, G. De Vita, DEPFET sensor with intrinsic signal compression developed for use at the XFEL free electron laser radiation source, Nucl. Instrum. Methods Phys. Res. A 624 (2) (2010) 528–532, http://dx.doi.org/10.1016/j.nima.2010.03.002.

[3] M. Porro, et al., The MiniSDD-based 1-Mpixel Camera of the DSSC Project for the European XFEL, IEEE Trans. Nucl. Sci. 68 (6) (2021) 1334–1350, http://dx.doi.org/10.1109/TNS.2021.3076602.

[4] W. Decking, et al., A MHz-repetition-rate hard X-ray free-electron laser driven by a superconducting linear accelerator, Nat. Photon. 14 (2020) 391–397, http://dx.doi.org/10.1038/s41566-020-0607-z.

[5] S. Aschauer, et al., First results on DEPFET Active Pixel Sensors fabricated in a CMOS foundry—a promising approach for new detector development and scientific instrumentation, JInst 12 (2017) P11013, http://dx.doi.org/10.1088/1748-0221/12/11/P11013.

[6] S. Maffessanti, et al., A 64k pixel CMOS-DEPFET module for the soft X-rays DSSC imager operating at MHz-frame rates, Sci. Rep. 13 (2023) 11799, http://dx.doi.org/10.1038/s41598-023-38508-9.

[7] A. Castoldi, et al., Calibration of the non-linear response of the first ladder of the DSSC camera with Soft X-rays at the European XFEL, in: 2022 IEEE Nuclear Science Symposium and Medical Imaging Conference (NSS/MIC), Vol. 13, 2022, pp. 1–3, http://dx.doi.org/10.1109/NSS/MIC44845.2022.10399245.